inorganics

MDPI

Article

Synthesis, X-ray Structures and Hirshfeld Analysis of Two Novel Thiocyanate-Bridged Ag(I) Coordination Polymers

Mezna Saleh Altowyan [1], Eman M. Fathalla [2,*], Jörg H. Albering [3], Morsy A. M. Abu-Youssef [2,*], Taher S. Kassem [2], Assem Barakat [4], Matti Haukka [5], Ahmed M. A. Badr [2] and Saied M. Soliman [2,*]

1 Department of Chemistry, College of Science, Princess Nourah bint Abdulrahman University, P.O. Box 84428, Riyadh 11671, Saudi Arabia; msaltowyan@pnu.edu.sa
2 Department of Chemistry, Faculty of Science, Alexandria University, Ibrahimia, P.O. Box 426, Alexandria 21321, Egypt; taher.kassem.2011@gmail.com (T.S.K.); ahmed_badr@alexu.edu.eg (A.M.A.B.)
3 Graz University of Technology, Mandellstr. 11/III, A-8010 Graz, Austria; joerg.albering@tugraz.at
4 Department of Chemistry, College of Science, King Saud University, P.O. Box 2455, Riyadh 11451, Saudi Arabia; ambarakat@ksu.edu.sa
5 Department of Chemistry, University of Jyväskylä, P.O. Box 35, FI-40014 Jyväskylä, Finland; matti.o.haukka@jyu.fi
* Correspondence: eman.nomeir@alexu.edu.eg (E.M.F.); morsy5@alexu.edu.eg (M.A.M.A.-Y.); saied1soliman@yahoo.com or saeed.soliman@alexu.edu.eg (S.M.S.)

Abstract: Two novel silver(I) coordination polymers, $[Ag(\mathbf{4BP})(SCN)]_n$ (**1**) and $\{(\mathbf{4BP}H)^+[Ag(SCN)_2]^-\}_n$ (**2**) (**4BP** = 4-benzoyl pyridine), have been synthesized. The two complexes were prepared using almost the same reagents, which were $AgNO_3$, **4BP** and NH_4SCN. The only difference was the presence of 1:1 (*v*/*v*) HNO_3 in the synthesis of **2**. In the two complexes, the Ag(I) has distorted tetrahedral coordination geometry. The structure of both complexes and the involvement of the thiocyanate anion as a linker between the Ag(I) centers were confirmed using single-crystal X-ray diffraction. **4BP** participated as a monodentate ligand in the coordination sphere of complex **1**, while in **2** it is found protonated (**4BP**-H)$^+$ and acts as a counter ion, which balances the charge of the anionic $[Ag(SCN)_2]^-$ moiety. The thiocyanate anion shows different coordination modes in the two complexes. In complex **1**, the thiocyanate anion exhibits a $\mu_{1,1,3}$ bridging mode, which binds three Ag(I) ions to build a boat-like ten-membered ring structure leading to a two-dimensional coordination polymer. In **2**, there are mixed $\mu_{1,1}$ and $\mu_{1,3}$ bridging thiocyanate groups, which form the one-dimensional polymeric chain running in the *a*-direction. Several interactions affected the stability of the crystal structure of the two complexes. These interactions were examined using Hirshfeld surface analysis. The coordination interactions (Ag-S and Ag-N) have a great impact on the stability of the polymeric structure of the two complexes. Additionally, the hydrogen-bonding interactions are crucial in the assembly of these coordination polymers. The O…H (10.7%) and C…H (34.2%) contacts in **1** as well as the N···H (15.3%) and S···H (14.9%) contacts in **2** are the most significant. Moreover, the argentophilic interaction (Ag…Ag = 3.378 Å) and π- π stacking play an important role in the assembly of complex **2**.

Keywords: AgSCN coordination polymer; 4-benzoyl pyridine; X-ray diffraction; supramolecular; Hirshfeld

Citation: Altowyan, M.S.; Fathalla, E.M.; Albering, J.H.; Abu-Youssef, M.A.M.; Kassem, T.S.; Barakat, A.; Haukka, M.; Badr, A.M.A.; Soliman, S.M. Synthesis, X-ray Structures and Hirshfeld Analysis of Two Novel Thiocyanate-Bridged Ag(I) Coordination Polymers. *Inorganics* **2023**, *11*, 417. https://doi.org/10.3390/inorganics11100417

Academic Editor: Jean Pierre Djukic

Received: 27 September 2023
Revised: 17 October 2023
Accepted: 19 October 2023
Published: 23 October 2023

1. Introduction

Coordination polymers (CPs) have gained prominence in the field of materials science. Due to their many potential applications, particularly in gas storage [1,2], separation [3,4], catalysis [5–7], sensors, optoelectronics [8,9], nanomaterial synthesis [10,11], illumination, photodetection [12,13] and drug delivery [14,15], CPs with one- to three-dimensional structures have been studied. In particular, silver is an effective metal to be used for the synthesis of CPs because it can involve coordination numbers ranging from 2 to 6,

providing a variety of coordination geometries [16]. Also, some Ag-CPs have coordination numbers greater than six [17,18]. Furthermore, the structural diversity of silver-based CPs is affected not only by the supramolecular Ag···ligand, Ag···C, Ag···π, C-H···π, H-bonds, π-π stacking and anion interactions [19–22] but also by the significant Ag···Ag interactions (argentophilicity) [23–25], which have an impact on the structural diversity and appealing optoelectronic properties [26–34]. As a result, silver is one of the top ten metals chosen to construct 2D CPs [35,36]. Moreover, 8% of all the CPs (1D–3D) in the MOF subset are Ag-CPs [37]. These materials were found to exhibit fascinating structural motifs [21,38–40] and intriguing properties, including electrical conductivity [41,42], photoluminescence [27,43], guest exchange and sorption [44,45], magnetism [46,47], catalysis [48,49], antitumor [50] as well as antibacterial activities [51]. More recently, Ag(I) compounds with N-heterocyclic ligands have been reported to show more cytotoxic action than *cis*-platin against tested cancer cell lines [52].

Pyridine derivatives are among the most often used nitrogen-containing heterocyclic ligands. Due to the variety of ligand design and the ability to form labile and reversible bonds, the metal–pyridine coordination bond is among the most ideal systems for the self-assembly of well-organized CPs [53–56]. Various factors should be taken into consideration for the successful preparation of these polymeric materials, including the reaction conditions [57], the ratio of silver to ligand [58], silver ion stereochemistry coupled with the functionality of the ligands [59] and the characteristics of counter-anions [60]. Recently, our research groups reported the synthesis and X-ray structure analysis combined with Hirshfeld and antimicrobial studies of polymeric $[Ag(3\text{-cyanopyridine})_2(CF_3COO)]_n$ and the dinuclear $[Ag(4\text{-benzoylpyridine})_2]_2(CF_3COO)_2$ complexes [61]. In addition, the X-ray structure of $[Ag(4\text{-benzoylpyridine})_2](NO_3).H_2O$ revealed the monomeric structure of this complex [62].

In this regard, thiocyanate (SCN^-) is frequently used as a bridging ligand for creating new silver clusters because of the strong Ag-S bond and the high ability of silver to form relatively stable coordination compounds with nitrogen a as donor atom [63–67], in addition to its various coordination modes (Figure 1) [68–75]. The crystal structure of the simple silver(I) thiocyanate salt has been reported by Zhu and coworkers. Its X-ray structure revealed a 3D network via Ag—S bonds and weak Ag. . .Ag interactions where each Ag-atom has a T-shaped coordination environment [65]. Also, the X-ray structure of the AgSCN adducts with pyridine and other heterocyclic ligands was reported in the literature to have an oligo-nuclear structure [67], i.e., 1-, 2- and 3D polymeric networks that use AgSCN fragments as their building blocks [65,73,74].

In the light of the interesting structural and supramolecular structure properties of Ag(I) thiocyanato complexes, we report herein the synthesis of two new Ag(I)-CPs with 4-benzoyl pyridine (**4BP**) (Figure 2), using thiocyanate as a linker. The structure of the synthesized complexes was verified using single-crystal X-ray diffraction analysis. In addition, Hirshfeld calculations were used to investigate the supramolecular architectures of the studied complexes.

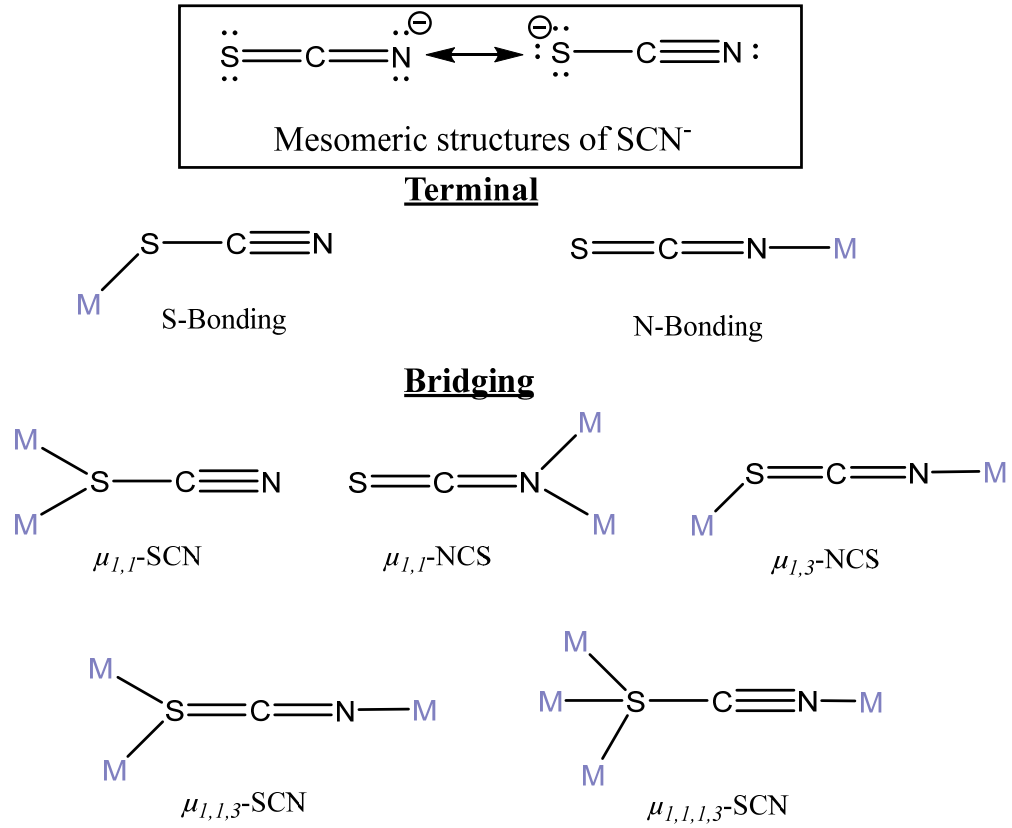

Figure 1. Mesomeric structures and coordination modes of SCN^- ion.

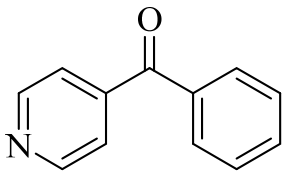

Figure 2. Structure of 4-benzoyl pyridine (**4BP**).

2. Results and Discussion

2.1. Synthesis and Characterizations

The X-ray structures of the Ag(I) complexes with 4-benzoylpyridine with different anions such as CF_3COO^- and NO_3^- were previously reported in the literature [61,62]. The former complex $[Ag(\mathbf{4BP})_2]_2(CF_3COO)_2$ is dinuclear through a strong argentophilic interaction connecting the two $[Ag(\mathbf{4BP})_2]$ cationic units [61] while the latter $[Ag(\mathbf{4BP})_2](NO_3).H_2O$ is monomeric [62]. In both cases, the 4-benzoylpyridine molecule is acting as a monodentate ligand via its pyridine N-atom, and no close contacts were found between the Ag(I) ion and the carbonyl group. For $[Ag(\mathbf{4BP})_2]_2(CF_3COO)_2$, the nonpolar C···H (26.2%) and the polar O···H (15.6%) interactions were found to be the most important in the molecular packing. In this work, we present the synthesis of two new Ag(I) complexes with 4-benzoylpyridine (**4BP**) in the presence of thiocyanate (SCN^-) as a bridging ligand. Schematic illustration for the synthesis of the two complexes is shown in Scheme 1. The two complexes were prepared using almost the same reagents, which are $AgNO_3$, **4BP** and NH_4SCN. The only difference is the addition of 1:1 (*v*/*v*) HNO_3 in the synthesis of **2**. After mixing, the resulting clear solutions were left for slow evaporation at room temperature. After a few days, both complexes were formed in crystalline forms, which are suitable for single-crystal X-ray diffraction analysis. Based on the CIF data, the Hirshfeld calculations were used to investigate the intermolecular interactions of the studied complexes.

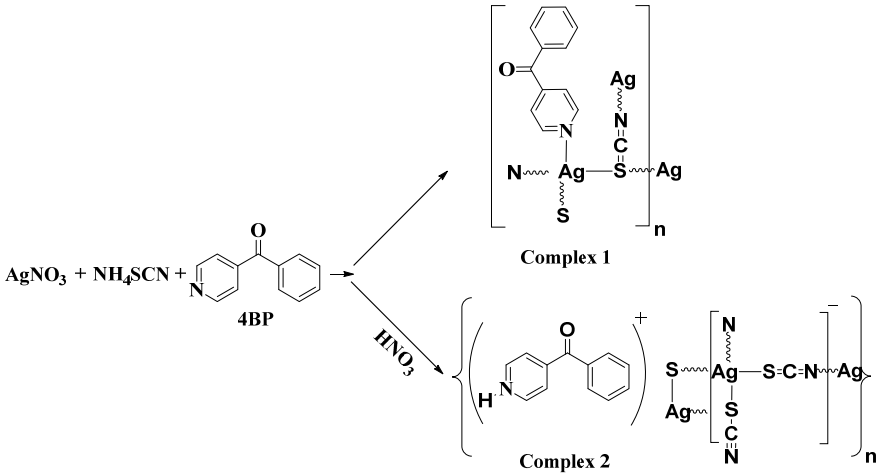

Scheme 1. Synthesis of the two complexes, **1** and **2**.

*2.2. X-ray Crystal Structure Description of [Ag(**4BP**)(SCN)]$_n$ (**1**)*

The structure of complex **1** has been revealed using single-crystal X-ray crystallography to be [Ag(**4BP**)(SCN)]$_n$. It crystallizes in the orthorhombic system with the *Pna2*$_1$ space group and Z = 4. The unit cell parameters are a = 27.2079(9) Å, b = 6.0833(2) Å and c = 7.5732(2) Å while the unit cell volume equals 1253.47(7) Å^3. The asymmetric unit consists of one [Ag**4BP**(SCN)] unit (Figure 3a). The structure of the title complex is approved to have a 2D polymeric structure via the Ag-N and Ag-S interactions between the Ag(I) and the bridged SCN$^-$ group.

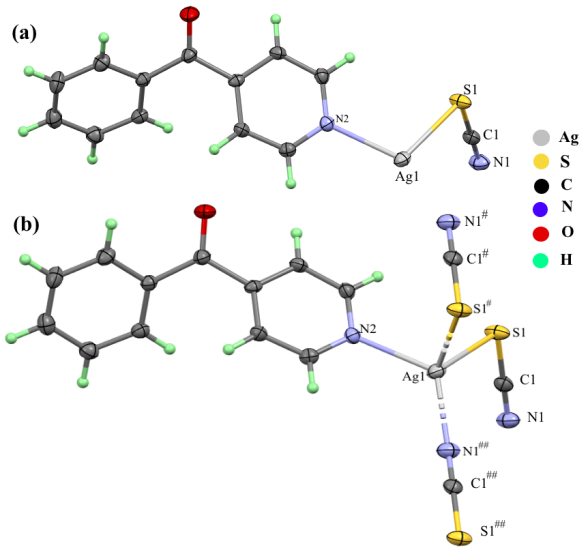

Figure 3. Structure of the asymmetric unit (**a**) and the complete coordination geometry around Ag(I) (**b**) in complex **1**. Symmetry codes for S1 $^{\#}$: 1 − x, 1 − y, −1/2 + z and for N1 $^{\#\#}$: 1 – x,2 – y, −1/2 + z.

In complex **1**, the Ag(I) is tetra-coordinated (Figure 3b) by one pyridine N-atom from the **4BP**; Ag1–N2; 2.331(2) Å, two thiocyanate sulfur atoms; Ag1–S1; 2.5885(8) Å, Ag1–S1$^{\#}$; 2.6136(8) Å and one nitrogen atom from another thiocyanate anion; Ag1–N1$^{\#\#}$; 2.175(3) Å. The bond angles inside the coordination sphere range from 93.98(6)° (N2-Ag1-S1$^{\#}$) to 123.35(10)° (N1-Ag1-N2). Hence, the coordination geometry around the Ag(I) is considered a distorted tetrahedron. Selected bond lengths and angles are given in Table 1. The Ag-N distances were found to be 2.1708(11) Å and 2.1733(12) Å in the [Ag(**4BP**)$_2$]$_2$(CF$_3$COO)$_2$ complex [61] and 2.146(3) Å and 2.147(3) Å in the [Ag(**4BP**)$_2$](NO$_3$).H$_2$O complex [62]. The Ag-N distances are shorter in these cases due to the absence of a coordinating anion attached to the Ag(I) ion.

Table 1. Selected bond lengths (Å) and angles (°) for **1**.

Bond	Distance	Bond	Distance
Ag1-N1$^{\#\#}$	2.175(3)	Ag1-S1	2.5885(8)
Ag1-N2	2.331(2)	Ag1-S1$^{\#}$	2.6136(8)
Bonds	**Angle**	**Bonds**	**Angle**
N1$^{\#\#}$-Ag1-N2	123.35(10)	C1-S1-Ag1	96.34(12)
N1$^{\#\#}$-Ag1-S1	116.58(8)	C1$^{\#}$-S1$^{\#}$-Ag1	94.97(11)
N2-Ag1-S1	103.91(7)	Ag1-S1-Ag1	155.04(4)
N1$^{\#\#}$-Ag1-S1$^{\#}$	115.60(8)	C1$^{\#\#}$-N1$^{\#\#}$-Ag1	158.2(3)
N2-Ag1-S1$^{\#}$	93.98(6)	C2-N2-Ag1	122.0(2)
S1-Ag1-S1$^{\#}$	98.727(10)	C6-N2-Ag1	118.59(19)

Symmetry codes: $^{\#}$ 1 − x, 1 − y, −1/2 − z and $^{\#\#}$ 1 − x,2 − y, −1/2 + z.

Each thiocyanate anion exhibits a $\mu_{1,1,3}$-*(S,S,N-)* bridging mode, which binds three Ag(I) centers leading to a boat-like ten-membered ring. These repeating units are fused together to generate a 2D wavy-like structure extended along the *ac* plane (Figure 4a). As a result, each sulfur atom connects two silver atoms, one from its own unit and the other from another adjacent unit, leading to zig-zag chains extended along the *c*-direction, where the Ag–S–Ag angle is 155.04(4)°. These polymeric chains are further connected by the coordination interaction between the Ag(I) ion and N-atom from the third thiocyanate group, which extends the coordination polymer along the *b*-direction leading to the 2D polymeric structure shown in Figure 4b. The angles of the thiocyanate groups are nearly linear (179.7(4)° and 158.2(3)° for S1–C1–N1 and C1$^{\#\#}$-N1$^{\#\#}$-Ag1, respectively) while the Ag1–S1–C1 acquires bent conformation, with angles 96.34(12)° for Ag1–S1–C1 and 94.97(11)° for Ag1–S1$^{\#}$–C1$^{\#}$. These results are consistent with the mesomeric structure of the thiocyanate group [69,75]. The **4BP** organic ligand acts as a terminal monodentate ligand via the pyridine N-atom and thus is not included in the polymer expansion but is found located above and below the polymeric zig-zag chains (Figure 5).

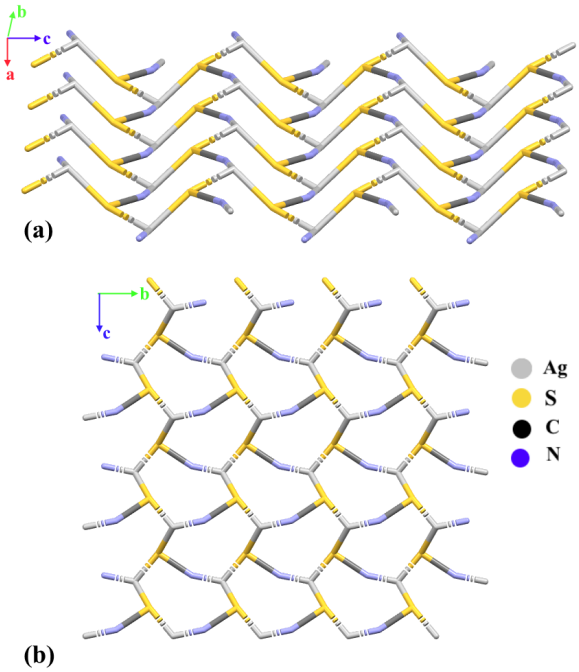

Figure 4. The zigzag-like (**a**) showing the two-dimensional polymeric structure (**b**) of complex **1** formed by the $\mu_{1,1,3}$-thiocyanate bridging ligand, viewed along two different axes. The **4BP** and H-atoms are omitted for clarity.

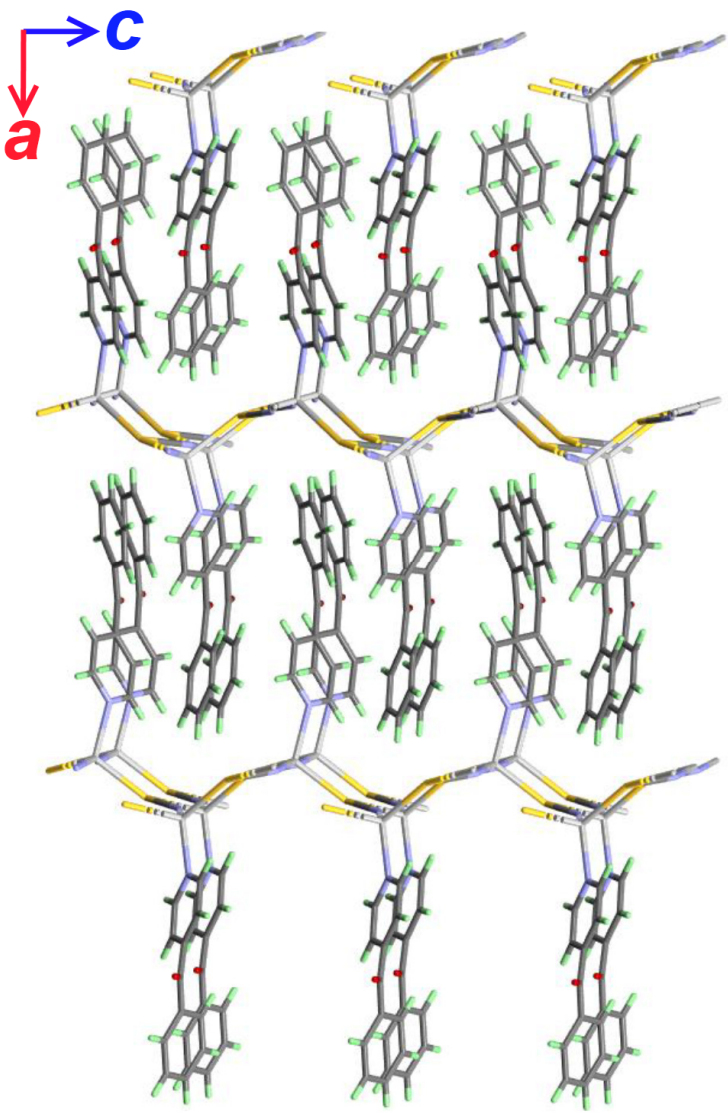

Figure 5. The monodentate **4BP** ligand units are found above and below the zig-zag chains of the 2D polymer.

*2.3. X-ray Crystal Structure Description of {(**4BP**-H)$^+$[Ag(SCN)$_2$]$^-$}$_n$ (**2**)*

The crystal structure of complex **2** consists of the anionic complex $[Ag(SCN)_2]^-$, which forms a one-dimensional polymeric structure, in addition to the protonated **4BP** cation (**4BP**-H)$^+$ as an outer sphere. The compound crystallizes in the triclinic system with the space group *P-1* and Z = 2. The unit cell parameters are a = 6.0975(2) Å, b = 8.7626(4) Å, c = 14.6204(6) Å, α = 95.010(2)° and β = 100.1270(10)° while the unit cell volume is 765.80(5) Å^3. The asymmetric unit and the coordination geometry of the Ag(I) together with the numbering scheme are shown in Figure 6. The asymmetric unit is composed of one **4BP**-H$^+$ and one $[Ag(SCN)_2]^-$ anion. In this complex, the N-atom (N3) from the **4BP** is found protonated and is not involved in any coordination interaction with the Ag(I) ion.

In the anionic part of this complex, the crystallographically unique Ag1 center is tetra-coordinated by four thiocyanate groups via the three S-atoms S1, S1$^{\#}$ and S2 in addition to the N-atom N2$^{\#\#}$. The S(1)C(1)N(1)$^-$ exhibit a $\mu_{1,1}$-mode while the S(2)C(2)N(2)$^-$ exhibit a $\mu_{1,3}$-mode. The main geometrical parameters of the $[Ag(SCN)_2]^-$ anion are depicted in Table 2. The Ag-S distances range from 2.5747(6) to 2.6788(7) Å while the Ag-N bond distance is 2.213(2) Å. The angles around the silver atom are in the range from 99.980(19)° to 132.38(8)°, revealing a distorted tetrahedral coordination geometry. As a result of the end-to-end ($\mu_{1,3}$-) bonding mode of the S(2)C(2)N(2)$^-$, the anionic part of the complex

formed a one-dimensional polymeric chain running along the *a*-direction while the two thiocyanate groups with the ($\mu_{1,1}$-) bonding mode bi-bridge two Ag(I) centers (Figure 7). As a result, the anionic chain can more easily be considered as a lengthwise stacking of the $[(Ag)_2(SCN)_2]^-$ dinuclear units. The Ag. . .Ag separation in the dinuclear unit is 3.379(4) Å, which is a little bit shorter than the sum of the van der Waals radii of two silver atoms (3.44 Å) [23], indicating weak argentophilic interactions, unlike the $[Ag(\mathbf{4BP})_2]_2(CF_3COO)_2$ complex in which the Ag-Ag distance is short 3.0740(2) Å, indicating a strong argentophilic interaction, which leads to the dinuclear complex.

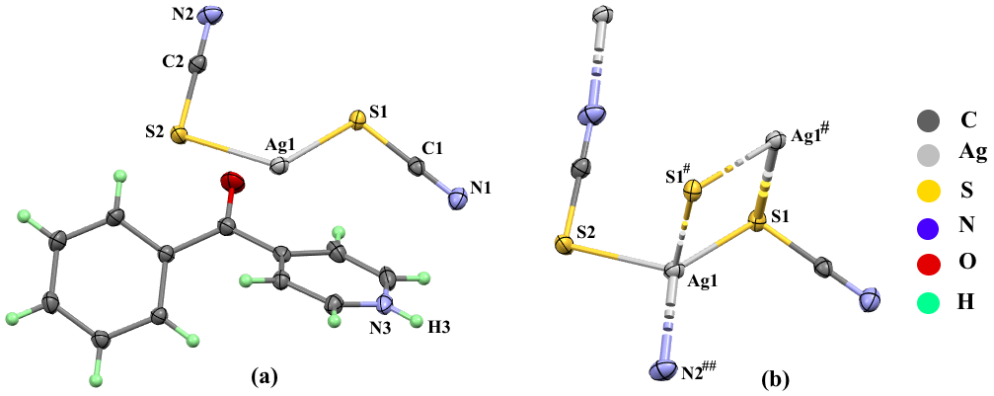

Figure 6. The asymmetric unit (**a**) and the coordination geometries of the silver (I) ion (**b**) in the polymeric structure of compound **2**. Symmetry codes: # 2 − x, −y, −z and ## −1 + x, y, z.

Table 2. Selected geometric parameters (Å, °) for complex **2**.

Bond	Distance	Bond	Distance
Ag1-N2$^{\#\#}$	2.213(2)	Ag1-S2	2.5890(8)
Ag1-S1	2.5747(6)	Ag1-S1$^{\#}$	2.6788(7)
Bonds	**Angle**	**Bonds**	**Angle**
N2$^{\#\#}$-Ag1-S1	132.38(8)	S2-Ag1-Ag1$^{\#}$	115.482(15)
N2$^{\#\#}$-Ag1-S2	106.15(7)	S1-Ag1$^{\#}$-Ag1	48.637(14)
S1-Ag1-S2	100.97(2)	C1-S1-Ag1	103.49(8)
N2$^{\#\#}$-Ag1-S1$^{\#}$	105.56(7)	C1-S1-Ag1$^{\#}$	98.38(9)
S1-Ag1-S1$^{\#}$	99.980(19)	Ag1-S1-Ag1	80.020(19)
S2-Ag1-S1$^{\#}$	111.08(2)	C2-S2-Ag1	97.88(9)
N2-Ag1-Ag1$^{\#}$	136.58(7)	C2-N2-Ag1$^{\#\#\#}$	172.9(2)
S1$^{\#}$-Ag1$^{\#}$-Ag1	51.343(15)		

Symmetry codes: # 2 − x, −y, −z, ## −1 + x, y, z and ### 1 + x, y, z.

The thiocyanates in **2** are slightly less linear compared to complex **1** as can be observed from the S1–C1–N1 and S2–C2–N2 angles [179.1(3)° and 177.7(3)°, respectively]. As evident, the order of deviation from the linearity (180°) of the SCN^- group according to its bonding mode is $\mu_{1,1,3} < \mu_{1,1} < \mu_{1,3}$.

The cationic part (**4BP**-H)$^+$ of complex **2** acts as the templating agent that fills the space between the 1D anionic polymer. On the other hand, the 2D supramolecular framework of the complex is constructed mainly via the C–H. . .S interactions. These interactions occur between the carbon atom (C7) of the pyridine moiety in the (**4BP**-H)$^+$ as the hydrogen bond donor and the $\mu_{1,1}$- thiocyanato S-atom (S1) as the hydrogen bond acceptor and between the C12-H12 from the phenyl moiety of the (**4BP**-H)$^+$ cation and S2 of the $\mu_{1,3}$- thiocyanato group (Figure 8). The C7. . .S1 and C12. . .S2 contact distances are 3.692 Å and 3.639 Å, respectively, while the H7. . .S1 and H12. . .S2 distances are 2.900 Å and 2.908 Å, respectively. Moreover, there is a significant N3-H3. . .N1 hydrogen-bonding interaction between the protonated N-atom (N3) of the (**4BP**-H)$^+$ as the hydrogen bond donor and the freely uncoordinated

N-atom (N1) from the $\mu_{1,1}$- thiocyanate group as the hydrogen bond acceptor (Figure 8). The H3. . .N1 and N3. . .N1 distances are 1.880 Å and 2.723 (3) Å, respectively.

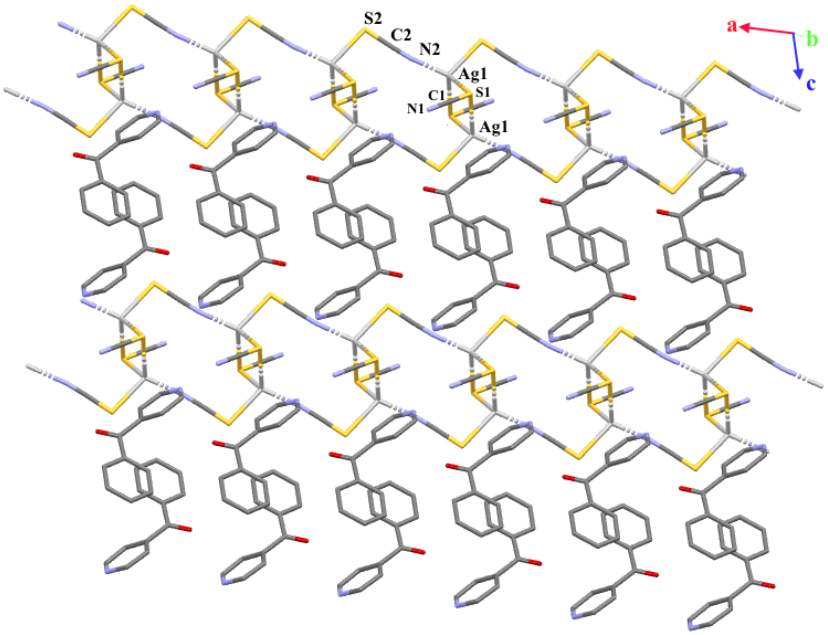

Figure 7. The 1D polymeric chain for the $[Ag(SCN)_2]^-$ along the a-axis with (**4BP**-H)$^+$ as the templating agent. Hydrogen atoms have been omitted for clarity.

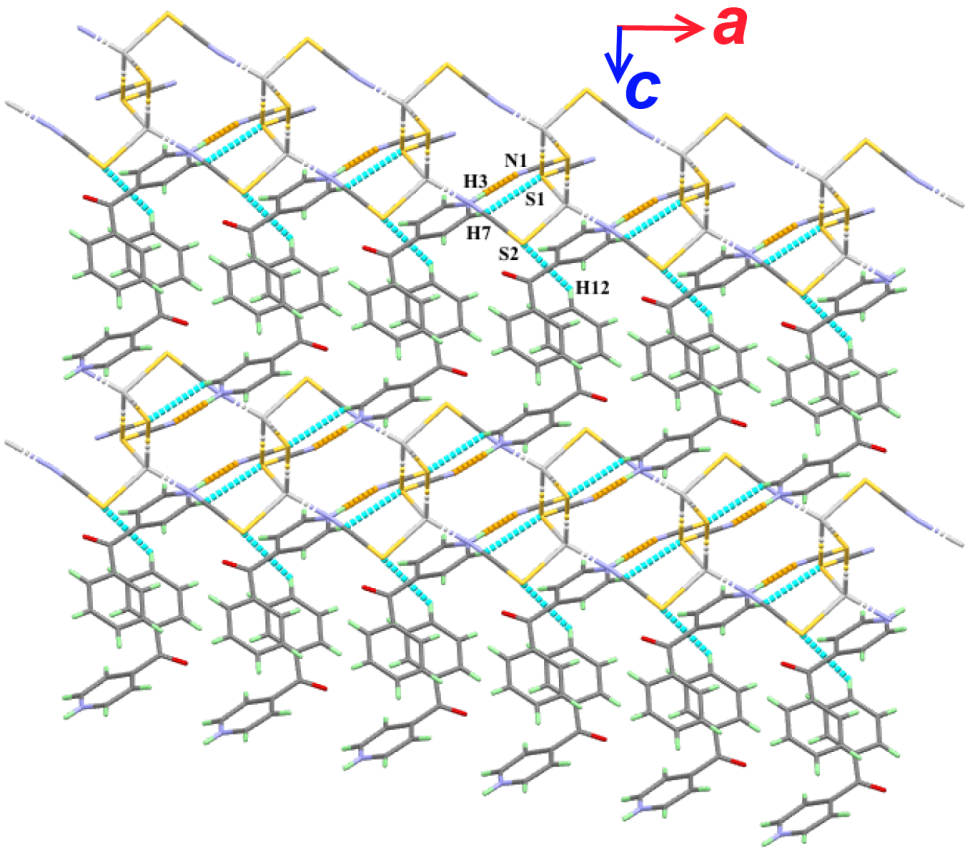

Figure 8. The 2D supramolecular sheet structure of {(**4BP**-H)$^+$[Ag(SCN)$_2$]$^-$}$_n$ (**2**). The turquoise and orange dotted lines refer to S. . .H and N. . .H interactions, respectively.

2.4. Analysis of Molecular Packing

The crystalline polymeric silver complexes **1** and **2** have a well-ordered arrangement that maintains the stability of the crystal through a set of interactions. These interactions involve primary bonds (covalent bonds) and secondary bonds (van der Waals, hydrogen bonds, Ag···Ag interactions, π-π stacking, etc.). A leading method for finding and analyzing all potential interactions that affect a crystal structure's stability is Hirshfeld topology analysis. Figure 9 shows the Hirshfeld surface mapped with the d_{norm} properties along with the neighboring molecules involved in the closest contacts. The red and blue areas in the d_{norm} map represent contacts shorter and longer than the sum of the van der Waals radii of the contacting atoms. Figure 10 illustrates the 2D fingerprint (FP) plots of the important interactions in the [Ag(**4BP**)(SCN)]$_n$ complex (**1**).

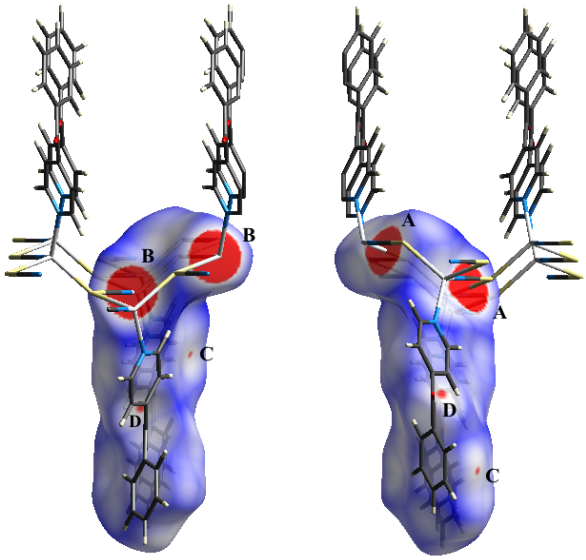

Figure 9. Full d_{norm} map for the [Ag(**4BP**)(SCN)]$_n$ (**1**). The most significant interactions are (A) Ag-S, (B) Ag-N, (C) C···H and (D) O···H.

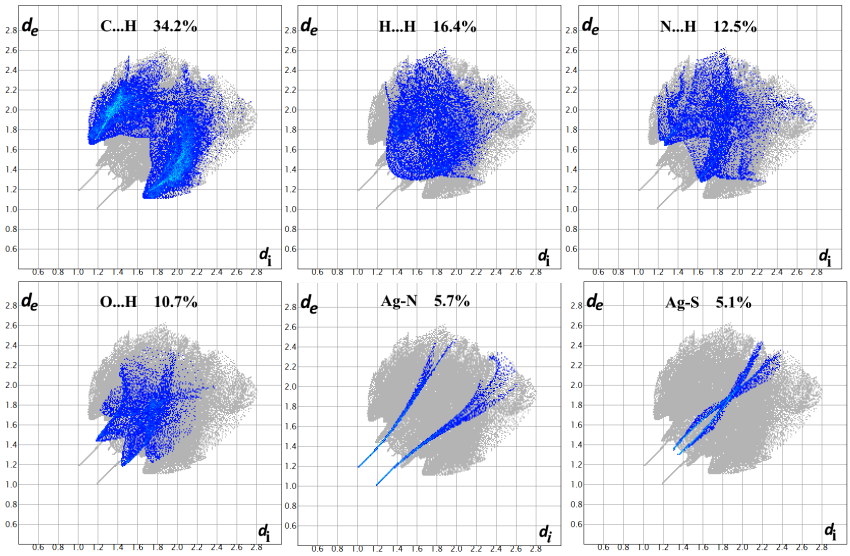

Figure 10. Hirshfeld 2D fingerprint plots for the most significant (Ag-N, Ag-S, O. . .H and C. . .H) interactions and other contacts (H. . .H and N. . .H), which have a high percentage in complex **1**.

The polymeric Ag-S (5.1%) and Ag-N (5.7%) interactions appear as intense red spots in the d_{norm} map (Figure 9) and as two distinct sharp spikes in the FP plot (Figure 10),

indicating that these coordination interactions have great significance for the extension of the polymeric chain structure and in the stability of complex **1** as well. Additionally, other contacts such as C. . .H and O. . .H are important for the crystal stability of complex **1**. These interactions represent 34.2% and 10.7% of the total Hirshfeld surface area for this complex. These interactions occur between the adjacent organic ligand (**4BP**) moieties. The C2. . .H9 and O1. . .H5 are the shortest interactions, where their corresponding distances are 2.741 Å and 2.592 Å, respectively.

Also, the supramolecular structure of the [Ag(**4BP**)(SCN)]$_n$ complex is affected by other numerous weak interactions. Figure 11 displays a summary of all contacts and their contributions to the molecular packing of this complex. The significant C. . .H (34.2%), hydrogenic H. . .H (16.4%) and N. . .H (12.5%) interactions are the most frequent interactions.

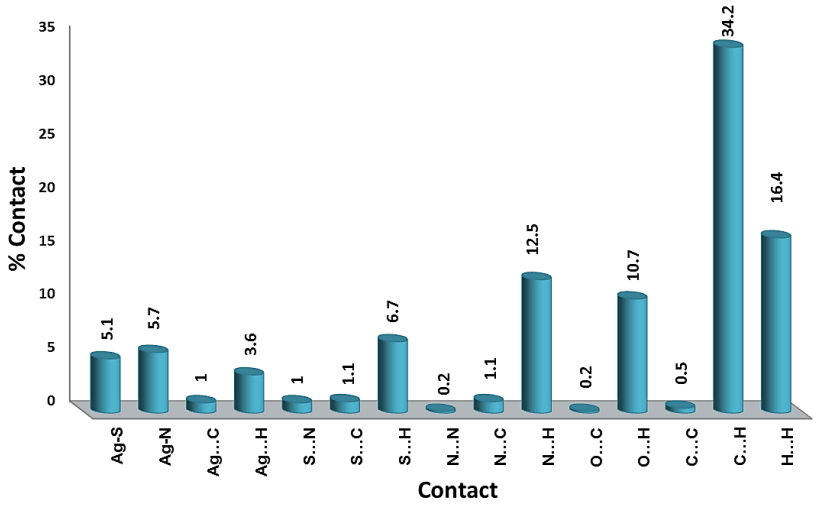

Figure 11. All the intermolecular interactions in [Ag(**4BP**)(SCN)]$_n$ (**1**).

For the compound {(**4BP**-H)$^+$[Ag(SCN)$_2$]$^-$}$_n$ (**2**), the d$_{norm}$ map and the 2D fingerprint plots are presented in Figures 12 and 13, respectively. As in **1**, the polymeric Ag-S and Ag-N interactions appear as intense red spots in the d$_{norm}$ map and as two distinct sharp spikes in the FP plot. Their respective contributions are 3.5% and 5.3%, respectively. It revealed the polymeric nature of this compound through coordination interactions between the Ag(I) ion and the thiocyanato sulfur and nitrogen atoms, which form the 1D polymeric chain of this complex. As shown in Figure 12, the d$_{norm}$ map shows other red spots related to the N. . .H, S. . .H, C. . .O and Ag. . .Ag contacts, which are also important for the crystal stability of complex **2**.

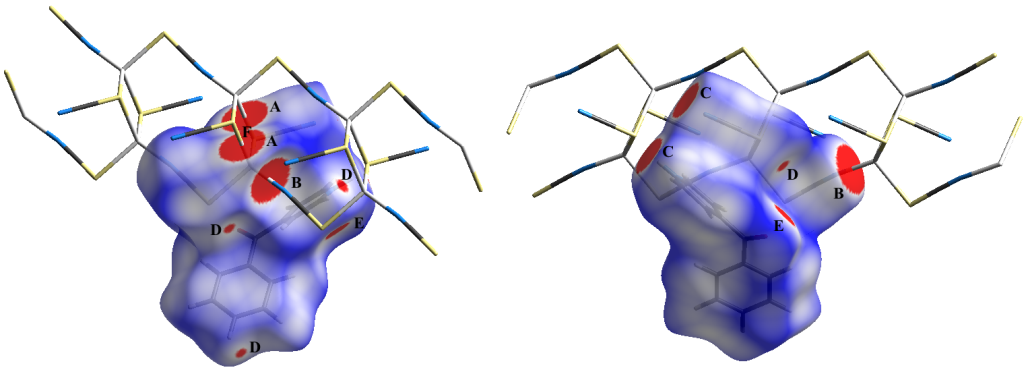

Figure 12. Full d$_{norm}$ map for the {(**4BP**-H)$^+$[Ag(SCN)$_2$]$^-$}$_n$ (**2**). The most significant interactions are (A) Ag-S, (B) Ag-N, (C) N···H, (D) S···H, (E) C. . .O and (F) Ag. . .Ag.

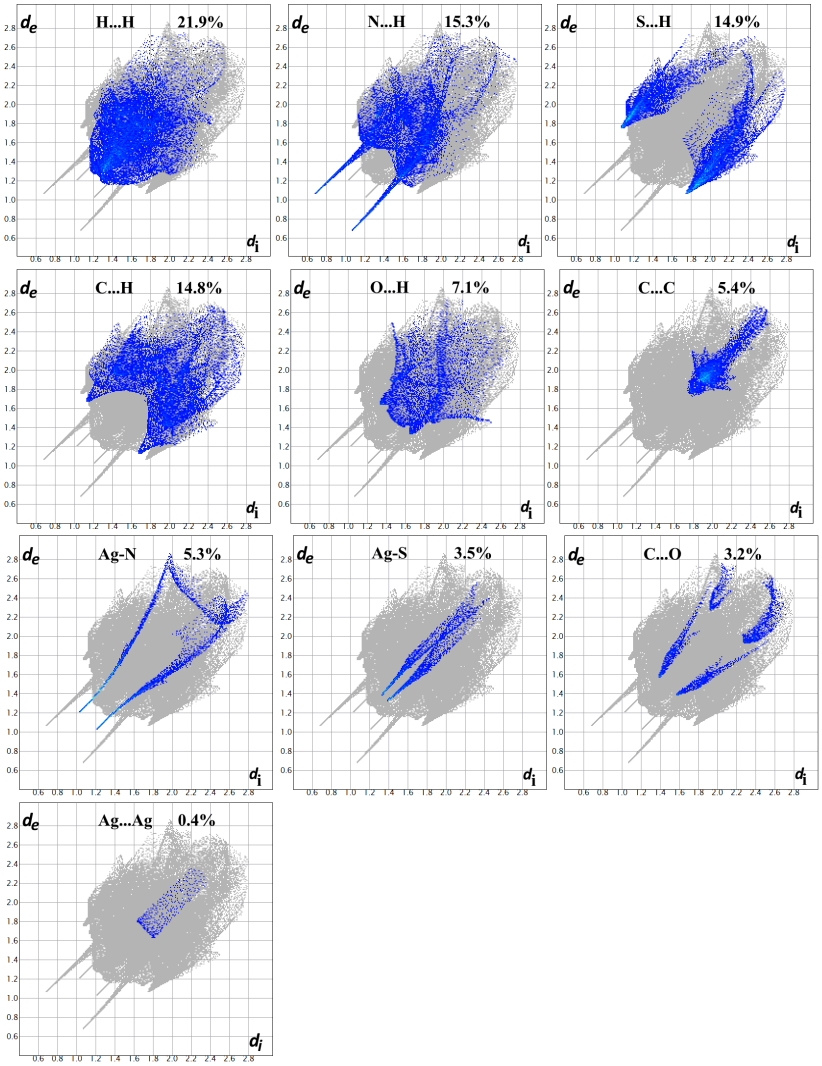

Figure 13. Hirshfeld 2D fingerprint plots of the most significant (Ag-N, Ag-S, N. . .H, S. . .H, C. . .O and Ag. . .Ag) interactions and other contacts (H. . .H, C. . .H, O. . .H and C. . .C) that contribute with a high percentage to the stability of complex **2**.

As shown in Figure 12, there are two large and intense red spots corresponding to the N. . .H interactions that also appear as sharp spikes in the FP plot (15.3%) (Figure 13), revealing the importance of this interaction in the crystal stability of **2**. The N. . .H interaction occurs between the uncoordinated N-atom (N1) of the $\mu_{1,1}$-thiocyanato group in the 1D polymeric chain of $[Ag(SCN)_2]^-$ anion and the hydrogen atom (H3) of the protonated **4BP** in (**4BP**-H)$^+$ cation where the N1. . .H3 distance is 1.734Å.

The S. . .H interaction appeared in the FP as wings and contributed to the crystal structure packing by 14.9%, indicating the importance of the interactions between the hydrogen atoms from the (**4BP**-H)$^+$ cation and the S-atoms of the $\mu_{1,1}$- (S1. . .H7 = 2.778 Å) and $\mu_{1,3}$-thiocyanato (S2. . .H12 = 2.798 Å) groups from the anionic complex part, leading to the extended 2D supramolecular framework. Moreover, the C. . .O interaction occurred between the adjacent (**4BP**-H)$^+$ cations where the C7. . .O2 distance is 2.916 Å. In addition, the argentophilic (Ag. . .Ag) interaction occurred in complex **2** (Ag1. . .Ag1 = 3.378 Å). On the other hand, the contribution of the C. . .C contact by 5.4% in the FP plot (Figure 13), along with the red/blue triangles and green flat area in the shape index (SI) and curvedness maps, respectively, confirm the existence of π- π stacking interactions between the parallel phenyl rings of the (**4BP**-H)$^+$ cation (Figure 14). The C11. . .C13 (3.712 Å) and C12. . .C12 (3.714 Å) are the shortest distances between the stacked phenyl rings. These distances are

longer than twice the van der Waals radii (3.40 Å) of the carbon atoms, indicating rather weak π-π stacking interactions.

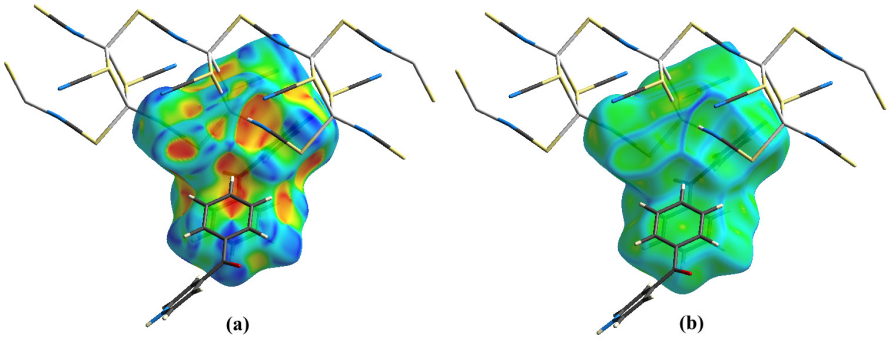

Figure 14. Full SI (**a**) and curvedness (**b**) maps for complex **2** showing the presence of the π-π interaction.

The other weak non-covalent interactions that occurred in complex **2** are shown in Figure 15. The hydrogenic H. . .H (21.9%), N. . .H (15.3%), S. . .H (14.9%) and C. . .H (14.8%) contacts were the most frequent interactions.

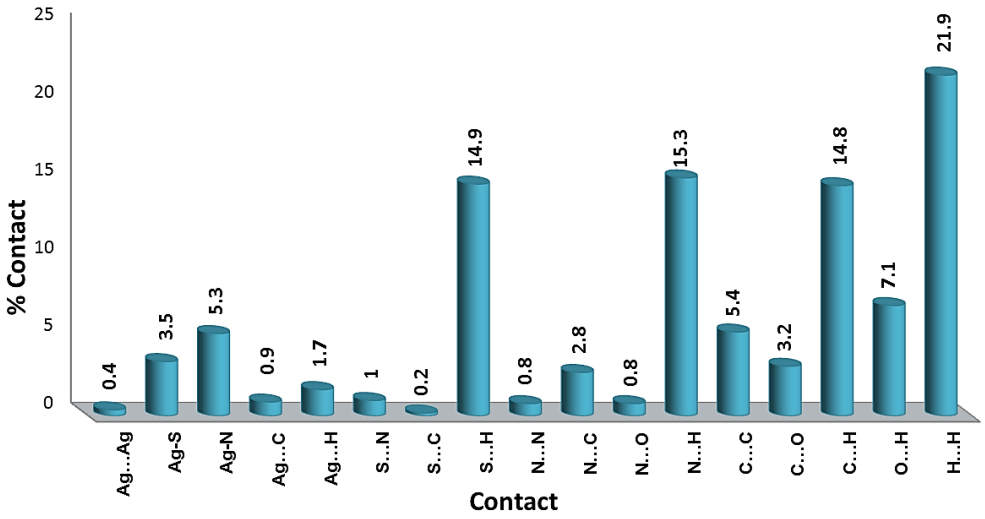

Figure 15. All the intermolecular interactions in {(**4BP**-H)$^{+}$[Ag(SCN)$_2$]$^{-}$}$_n$ (**2**).

3. Experimental

3.1. Material and Instrumentation

All chemicals were obtained from Sigma-Aldrich Company and used as received. A Perkin Elmer 2400 Elemental Analyzer (PerkinElmer, New York, NY, USA) was used to perform the CHN analyses. Additionally, the amount of Ag was determined using a Shimadzu atomic absorption spectrophotometer (AA-7000 series, Shimadzu, Ltd., Kyoto, Japan).

*3.2. Synthesis of the AgSCN/**4BP** CPS*

3.2.1. Synthesis of [Ag(**4BP**)(SCN)]$_n$ Complex (**1**)

An aqueous solution of silver(I) nitrate (170 mg, 1 mmol) in 10 mL was mixed with a saturated solution of ammonium thiocyanate followed by the addition of an ethanolic solution (10 mL) of **4BP** (183.2 mg, 1 mmol). This mixture was left at room temperature and allowed to evaporate slowly. Complex **1** was obtained as pale-yellow block crystals after 10 days. [Ag(**4BP**)(SCN)]$_n$ (**1**); (76% yield). Anal. Calc. $C_{13}H_9AgN_2OS$: C, 44.72; H, 2.60; N, 8.02; Ag, 30.89%. Found: C, 44.59; H, 2.56; N, 7.94; Ag, 30.71%.

3.2.2. Synthesis of $\{(\mathbf{4BP}\text{-H})^{+}[Ag(SCN)2]^{-}\}_{n}$ Complex (**2**)

An aqueous solution of silver(I) nitrate (170 mg, 1 mmol) in 10 mL was mixed with a saturated solution of ammonium thiocyanate followed by the addition of an ethanolic solution (10 mL) of **4BP** (183.2 mg, 1 mmol). To the resulting mixture, 2 mL of 1:1 (*v/v*) aqueous solution of nitric acid was added. Complex **2** was obtained as colorless needle crystals after 6 days. $\{(\mathbf{4BP}\text{-H})^{+}[Ag(SCN)_2]^{-}\}_{n}$ (**2**); (71% yield). Anal. Calc. $C_{14}H_{10}AgN_3OS_2$: C, 41.19; H, 2.47; N, 10.29; Ag, 26.42%. Found: C, 41.07; H, 2.44; N, 10.20; Ag, 26.29%.

3.3. X-ray Crystallography

The crystal structure of the two complexes was measured with the aid of Bruker APEX II machine employing graphite monochromator and MoKα radiation. Absorption corrections were performed using SADABS while all steps performed to solve the structure were executed using the SHELXTL program package [76]. Table S1 (Supplementary Data) provides a summary of the crystallographic results.

3.4. Hirshfeld Surface Analysis

The program Crystal Explorer 17.5 [77] was used to analyze the various intermolecular interactions in the investigated silver complexes.

4. Conclusions

The supramolecular structures of the 2D $[Ag(\mathbf{4BP})(SCN)]_{n}$ **(1)** and 1D $\{(\mathbf{4BP}\text{-H})^{+}[Ag(SCN)_2]^{-}\}_{n}$ (**2**) coordination polymers are presented. Both complexes were prepared from the reaction of 4-benzoyl pyridine (**4BP**) with $AgNO_3$ in the presence of thiocyanate as a linker. As shown from the X-ray structure analysis of both complexes, the **4BP** does not participate in expanding the polymeric structure. In complex **1**, it acts as a N-donor monodentate ligand while in **2** it does not participate in coordination and was found monoprotonated $(\mathbf{4BP}\text{-H})^{+}$. The thiocyanate anion displays different coordination modes in complexes **1** and **2**, which affects the interconnection of the $(AgSCN)_n$ fragments and the propagation of the network structure in the different dimensions. In the case of complex **1**, the SCN^{-} exhibits a $\mu_{1,13}$- bonding mode, while in **2** there are two types of bonding modes, which are the $\mu_{1,1}$- and $\mu_{1,3}$-types. As a result, 2D and 1D polymeric structures are obtained for complexes **1** and **2**, respectively. The supramolecular structure aspects of both complexes were analyzed quantitatively using Hirshfeld analysis. The non-covalent C. . .H and O. . .H interactions are the most significant contacts in **1** where the percentages of these interactions are 34.2% and 10.7%, respectively. In **2**, the N. . .H (15.3%), S. . .H (14.9%) and C. . .O (3.2%) contacts are the most significant. Additionally, the hydrogenic H. . .H interactions largely contributed to the packing of complexes **1** (16.4%) and **2** (21.9%).

Supplementary Materials: The following supporting information can be downloaded at: https://www.mdpi.com/article/10.3390/inorganics11100417/s1, Table S1: Crystal data and structure refinement for complexes **1** and **2**.

Author Contributions: Conceptualization, S.M.S. and M.A.M.A.-Y.; methodology, E.M.F., J.H.A., A.M.A.B., T.S.K. and A.B.; software, S.M.S., A.M.A.B., M.H. and A.B.; formal analysis, E.M.F., M.H. and A.M.A.B.; investigation, S.M.S., A.M.A.B., T.S.K. and E.M.F. resources, M.A.M.A.-Y. and A.B.; writing—original draft preparation, S.M.S., E.M.F., M.A.M.A.-Y., A.M.A.B. and A.B.; writing—review and editing, S.M.S., E.M.F., M.A.M.A.-Y., A.M.A.B. and A.B.; supervision, S.M.S. and M.A.M.A.-Y.; project administration, M.S.A.; funding acquisition, M.S.A. All authors have read and agreed to the published version of the manuscript.

Funding: Princess Nourah bint Abdulrahman University Researchers Supporting Project number (PNURSP2023R86), Princess Nourah bint Abdulrahman University, Riyadh, Saudi Arabia.

Data Availability Statement: Not applicable.

Acknowledgments: Princess Nourah bint Abdulrahman University Researchers Supporting Project number (PNURSP2023R86), Princess Nourah bint Abdulrahman University, Riyadh, Saudi Arabia.

Conflicts of Interest: The authors declare no conflict of interest.

References

1. Blagojević, V.A.; Lukić, V.; Begović, N.N.; Maričić, A.M.; Minić, D.M. Hydrogen Storage in a Layered Flexible $[Ni_2(btc)(en)_2]_n$ Coordination Polymer. *Int. J. Hydrogen Energy* **2016**, *41*, 22171–22181. [CrossRef]
2. Suh, M.P.; Park, H.J.; Prasad, T.K.; Lim, D.W. Hydrogen storage in metal–organic frameworks. *Chem. Rev.* **2012**, *112*, 782–835. [CrossRef] [PubMed]
3. Qiu, S.; Xue, M.; Zhu, G. Metal–organic framework membranes: From synthesis to separation application. *Chem. Soc. Rev.* **2014**, *43*, 6116–6140. [CrossRef] [PubMed]
4. Li, J.R.; Kuppler, R.J.; Zhou, H.C. Selective gas adsorption and separation in metal–organic frameworks. *Chem. Soc. Rev.* **2009**, *38*, 1477–1504. [CrossRef]
5. Wu, X.Y.; Qi, H.X.; Ning, J.J.; Wang, J.F.; Ren, Z.G.; Lang, J.P. One Silver(I)/Tetraphosphine Coordination Polymer Showing Good Catalytic Performance in the Photodegradation of Nitroaromatics in Aqueous Solution. *Appl. Catal. B Environ.* **2015**, *168–169*, 98–104. [CrossRef]
6. Xing, B.; Choi, M.F.; Xu, B. Design of Coordination Polymer Gels as Stable Catalytic Systems. *Chem.—Eur. J.* **2002**, *8*, 5028–5032. [CrossRef]
7. Maurya, M.R.; Kumar, A. Oxovanadium(IV) Based Coordination Polymers and Their Catalytic Potentials for the Oxidation of Styrene, Cyclohexene and Trans-Stilbene. *J. Mol. Catal. A Chem.* **2006**, *250*, 190–198. [CrossRef]
8. Liu, J.Q.; Luo, Z.D.; Pan, Y.; Singh, A.K.; Trivedi, M.; Kumar, A. Recent developments in luminescent coordination polymers: Designing strategies, sensing application and theoretical evidences. *Coord. Chem. Rev.* **2020**, *406*, 213145. [CrossRef]
9. Liu, H.; Wang, Y.; Qin, Z.; Liu, D.; Xu, H.; Dong, H.; Hu, W. Electrically conductive coordination polymers for electronic and optoelectronic device applications. *J. Phys. Chem. Lett.* **2021**, *12*, 1612–1630. [CrossRef]
10. Mirtamizdoust, B. Sonochemical Synthesis of Nano Lead(II) Metal-Organic Coordination Polymer; New Precursor for the Preparation of Nano-Materials. *Ultrason. Sonochem.* **2017**, *35*, 263–269. [CrossRef]
11. Molaei, F.; Bigdeli, F.; Morsali, A.; Joo, S.W.; Bruno, G.; Rudbari, H.A. Synthesis and Characterization of Different Zinc(II) Oxide Nano-Structures from Two New Zinc(II)- Quinoxaline Coordination Polymers. *J. Mol. Struct.* **2015**, *1095*, 8–14. [CrossRef]
12. San Sebastian, E.; Rodríguez-Diéguez, A.; Seco, J.M.; Cepeda, J. Coordination Polymers with Intriguing Photoluminescence Behavior: The Promising Avenue for Greatest Long- Lasting Phosphors. *Eur. J. Inorg. Chem.* **2018**, *2018*, 2155–2174. [CrossRef]
13. Li, Q.; Qian, J.; Zhou, J.; Du, L.; Zhao, Q. Highly chemically and thermally stable lanthanide coordination polymers for luminescent probes and white light emitting diodes. *CrystEngComm* **2020**, *22*, 2667–2674. [CrossRef]
14. Begum, S.; Hassan, Z.; Bräse, S.; Wöll, C.; Tsotsalas, M. Metal–organic framework-templated biomaterials: Recent progress in synthesis, functionalization, and applications. *Acc. Chem. Res.* **2019**, *52*, 1598–1610. [CrossRef] [PubMed]
15. Giménez-Marqués, M.; Hidalgo, T.; Serre, C.; Horcajada, P.J.C.C.R. Nanostructured metal–organic frameworks and their bio-related applications. *Coord. Chem. Rev.* **2016**, *307*, 342–360. [CrossRef]
16. Zhu, H.; Liu, D.; Li, Y.H.; Cui, G.H. A 1D Silver(I) Coordination Polymer as Luminescent Probe for Cu^{2+} and Effective Photocatalyst for Degradation Organic Dyes. *Inorg. Chem. Commun.* **2019**, *108*, 107539. [CrossRef]
17. Dinh Do, N.; Kovalchukova, O.; Stash, A.; Strashnova, S. Catena-Poly[Ammonium [Aquabis(μ-2,3,5,6-Tetraoxo-4-Nitropyridin-4-Ido) Argentate(I)]]. *Acta Crystallogr. Sect. E Struct. Rep. Online* **2013**, *69*, m477–m478. [CrossRef]
18. Fang, X.Q.; Deng, Z.P.; Huo, L.H.; Wan, W.; Zhu, Z.B.; Zhao, H.; Gao, S. New Family of Silver(I) Complexes Based on Hydroxyl and Carboxyl Groups Decorated Arenesulfonic Acid: Syntheses, Structures, and Luminescent Properties. *Inorg. Chem.* **2011**, *50*, 12562–12574. [CrossRef]
19. Chen, C.L.; Kang, B.S.; Su, C.Y. Recent Advances in Supramolecular Design and Assembly of Silver(I) Coordination Polymers. *Aust. J. Chem.* **2006**, *59*, 3–18. [CrossRef]
20. Capel Berdiell, I.; Warriner, S.L.; Halcrow, M.A. Silver(I) Complexes of Bis- and Tris- (Pyrazolyl)Azine Derivatives-Dimers, Coordination Polymers and a Pentametallic Assembly. *Dalton Trans.* **2018**, *47*, 5269–5278. [CrossRef]
21. Khlobystov, A.N.; Blake, A.J.; Champness, N.R.; Lemenovskii, D.A.; Majouga, A.G.; Zyk, N.V.; Schröder, M. Supramolecular Design of One-Dimensional Coordination Polymers Based on Silver(I) Complexes of Aromatic Nitrogen-Donor Ligands. *Coord. Chem. Rev.* **2001**, *222*, 155–192. [CrossRef]
22. Moghadam, Z.; Akhbari, K.; Jamali, F.; Shahangi Shirazi, F. All Procedures for the Synthesis of Silver Nanosheets. *Nanochem. Res.* **2017**, *2*, 248–260.
23. Schmidbaur, H.; Schier, A. Argentophilic interactions. *Angew. Chem. Int. Ed.* **2015**, *54*, 746–784. [CrossRef] [PubMed]
24. Sun, D.; Wang, H.; Lu, H.F.; Feng, S.Y.; Zhang, Z.W.; Sun, G.X.; Sun, D.F. Two birds with one stone: Anion templated ball-shaped Ag_{56} and disc-like Ag_{20} clusters. *Dalton Trans.* **2013**, *42*, 6281–6284. [CrossRef]
25. Sun, D.; Zhang, L.L.; Lu, H.F.; Feng, S.Y.; Sun, D.F. Brightyellow to orange-red thermochromic luminescence of an $Ag^{I}_{6}-Zn^{II}_{2}$ heterometallic aggregate. *Dalton Trans.* **2013**, *42*, 3528–3532. [CrossRef]
26. Lamming, G.; Kolokotroni, J.; Harrison, T.; Penfold, T.J.; Clegg, W.; Waddell, P.G.; Probert, M.R.; Houlton, A. Structural diversity and argentophilic interactions in one-dimensional silverbased coordination polymers. *Cryst. Growth Des.* **2017**, *17*, 5753–5763. [CrossRef]
27. Huang, R.W.; Wei, Y.S.; Dong, X.Y.; Wu, X.H.; Du, C.X.; Zang, S.Q.; Mak, T.C. Hypersensitive dual-function luminescence switching of a silver-chalcogenolate cluster based metal-organic framework. *Nat. Chem.* **2017**, *9*, 689. [CrossRef]

28. Xi, X.; Liu, Y.; Cui, Y. Homochiral Silver-Based Coordination Polymers Exhibiting Temperature-Dependent Photoluminescence Behavior. *Inorg. Chem.* **2014**, *53*, 2352–2354. [CrossRef]
29. Song, Y.F.; Abbas, H.; Ritchie, C.; McMillian, N.; Long, D.L.; Gadegaard, N.; Cronin, L. From polyoxometalate building blocks to polymers and materials: The silver connection. *J. Mater. Chem.* **2007**, *17*, 1903–1908. [CrossRef]
30. Rais, D.; Yau, J.; Mingos, D.M.P.; Vilar, R.; White, A.J.; Williams, D.J. Anion-Templated Syntheses of Rhombohedral Silver− Alkynyl Cage Compounds. *Angew. Chem. Int. Ed.* **2001**, *40*, 3464–3467. [CrossRef]
31. Liu, C.; Li, T.; Abroshan, H.; Li, Z.; Zhang, C.; Kim, H.J.; Li, G.; Jin, R. Chiral Ag_{23} nanocluster with open shell electronicstructure and helical face-centered cubic framework. *Nat. Commun.* **2018**, *9*, 744. [CrossRef] [PubMed]
32. Song, X.-R.; Goswami, N.; Yang, H.-H.; Xie, J. Functionalization of metal nanoclusters for biomedical applications. *Analyst* **2016**, *141*, 3126–3140. [CrossRef] [PubMed]
33. Zhang, S.S.; Su, H.F.; Zhuang, G.L.; Wang, X.P.; Tung, C.H.; Sun, D.; Zheng, L.S. A hexadecanuclear silver alkynyl clusterbased NbO framework with triple emissions from the visible to near-infrared II region. *Chem. Commun.* **2018**, *54*, 11905–11908. [CrossRef] [PubMed]
34. Chai, J.; Yang, S.; Lv, Y.; Chen, T.; Wang, S.; Yu, H.; Zhu, M. A unique pair: Ag_{40} and Ag_{46} nanoclusters with the same surface but different cores for structure—property correlation. *J. Am. Chem. Soc.* **2018**, *140*, 15582–15585. [CrossRef] [PubMed]
35. Morsali, A.; Hashemi, L. *Main Group Metal Coordination Polymers: Stuctures and Nanostructures*; John Wiley & Sons: Hoboken, NJ, USA, 2017.
36. Tran, M.; Kline, K.; Qin, Y.; Shen, Y.; Green, M.D.; Tongay, S. 2D Coordination Polymers: Design Guidelines and Materials Perspective. *Appl. Phys. Rev.* **2019**, *6*, 041311–041328. [CrossRef]
37. Allen, F.H. The Cambridge Structural Database: A Quarter of a Million Crystal Structures and Rising. *Acta Crystallogr. Sect. B* **2002**, *58*, 380–388. [CrossRef]
38. Su, C.Y.; Chen, C.L.; Zhang, J.Y.; Kang, B.S. Silver(I) coordination polymers. *Des. Constr. Coord. Polym.* **2009**, *5*, 111–144.
39. Steel, P.J.; Fitchett, C.M. Metallosupramolecular silver(I) assemblies based on pyrazine and related ligands. *Coord. Chem. Rev.* **2008**, *252*, 990–1006. [CrossRef]
40. Mak, T.C.; Zhao, X.-L. Silver: Inorganic and coordination chemistry. In *Encyclopedia of Inorganic and Bioinorganic Chemistry*; King, R.B., Ed.; John Wiley & Sons, Inc.: Chichester, UK, 2005; pp. 5187–5197.
41. Rana, A.; Jana, S.K.; Pal, T.; Puschmann, H.; Zangrando, E.; Dalai, S. Electrical conductivity and luminescence properties of two silver(I) coordination polymers with heterocyclic nitrogen ligands. *J. Solid State Chem.* **2014**, *216*, 49–55. [CrossRef]
42. Zheng, X.-F.; Zhu, L.-G. Synthesis, structures and conductivity properties of silver 3-sulfobenzoate coordination polymers. *Inorg. Chim. Acta* **2011**, *365*, 419–429. [CrossRef]
43. Yan, J.; Wilbraham, L.; Basa, P.N.; Schüttel, M.; Macdonald, J.C.; Ciofini, I.; Coudert, F.-X.; Burdette, S.C. Emissive azobenzenes delivered on a silver coordination polymer. *Inorg. Chem.* **2018**, *57*, 15009–15022. [CrossRef] [PubMed]
44. May, L.J.; Shimizu, G.K.H. Highly selective intercalation of primary amines in a continuous layer Ag coordination network. *Chem. Mater.* **2005**, *17*, 217–220. [CrossRef]
45. Yang, G.; Raptis, R.G. A robust, porous, cationic silver(I) 3,5-diphenyl-1,2,4-triazolate framework with a uninodal $4^9.6^6$ net. *Chem. Commun.* **2004**, *18*, 2058–2059. [CrossRef] [PubMed]
46. Yamada, S.; Ishida, T.; Nogami, T. Supramolecular triangular and linear arrays of metal-radical solids using pirazolato-silver(I) motifs. *Dalton Trans.* **2004**, *6*, 898–903. [CrossRef] [PubMed]
47. Rigamonti, L.; Vaccari, M.; Roncaglia, F.; Baschieri, C.; Forni, A. New silver(I) coordination polymer with Fe_4 single-molecule magnets as long spacer. *Magnetochemistry* **2018**, *4*, 43. [CrossRef]
48. Zhou, Z.; He, C.; Yang, L.; Wang, Y.; Liu, T.; Duan, C. Alkyne activation by a porous silver coordination polymer for heterogeneous catalysis of carbon dioxide cycloaddition. *ACS Catal.* **2017**, *7*, 2248–2256. [CrossRef]
49. Wang, C.C.; Jing, H.P.; Wang, P. Three silver-based complexes constructed from organic carboxylic acid and 4,4′-bipyridine-like ligands: Syntheses, structures and photocatalytic properties. *J. Mol. Struct.* **2014**, *1074*, 92–99. [CrossRef]
50. Sulaiman, N.I.; Salimin, N.R.; Haque, R.A.; Iqbal, M.A.; Ng, S.W.; Razali, M.R. Synthesis, spectroscopic characterization, single crystal X-ray determination and cytotoxicity activity against human breast cancer (MCF-7) and colon cancer (HCT 116) cell lines of silver (I) coordination polymer. *Polyhedron* **2015**, *97*, 188–196. [CrossRef]
51. Rogovoy, M.I.; Berezin, A.S.; Kozlova, Y.N.; Samsonenko, D.G.; Artem'ev, A.V. A layered Ag (I)-based coordination polymer showing sky-blue luminescence and antibacterial activity. *Inorg. Chem. Commun.* **2019**, *108*, 107513. [CrossRef]
52. El-Naggar, M.A.; Albering, J.H.; Barakat, A.; Abu-Youssef, M.A.; Soliman, S.M.; Badr, A.M. New bioactive 1D Ag (I) coordination polymers with pyrazole and triazine ligands; Synthesis, X-ray structure, Hirshfeld analysis and DFT studies. *Inorg. Chim. Acta* **2022**, *537*, 120948. [CrossRef]
53. Adarsh, N.N.; Dastidar, P. Coordination polymers: What has been achieved in going from innocent 4, 4′-bipyridine to bis-pyridyl ligands having a non-innocent backbone? *Chem. Soc. Rev.* **2012**, *41*, 3039–3060. [CrossRef] [PubMed]
54. Liu, Z.; Qayyum, M.F.; Wu, C.; Whited, M.T.; Djurovich, P.I.; Hodgson, K.O.; Hedman, B.; Solomon, E.I.; Thompson, M.E. A Codeposition route to CuI- pyridine coordination complexes for organic light-emitting diodes. *J. Am. Chem. Soc.* **2011**, *133*, 3700–3703. [CrossRef] [PubMed]

55. Abu-Youssef, M.A.M.; Langer, V.; Barakat, A.; Haukka, M.; Soliman, S.M. Molecular, Supramolecular Structures Combined with Hirshfeld and DFT Studies of Centrosymmetric M(II)-azido {M = Ni(II), Fe(II) or Zn(II)} Complexes of 4-Benzoylpyridine. *Symmetry* **2021**, *13*, 2026. [CrossRef]
56. Pai, S.; Schott, M.; Niklaus, L.; Posset, U.; Kurth, D.G. A study of the effect of pyridine linkers on the viscosity and electrochromic properties of metallo-supramolecular coordination polymers. *J. Mater. Chem. C* **2018**, *6*, 3310–3321. [CrossRef]
57. Blake, A.J.; Champness, N.R.; Cooke, P.A.; Nicolson, J.E.B. Synthesis of a chiral adamantoid network—the role of solvent in the construction of new coordination netwroks with silver(I). *Chem. Commun.* **2000**, *8*, 665–666. [CrossRef]
58. Feazell, R.P.; Carson, C.R.; Klausmeyer, K.K. Silver(I) 3-aminomethylpyridine complexes, Part 1: Effect of ligand ratio, π-stacking, and temperature with a noninteracting anion. *Inorg. Chem.* **2006**, *45*, 2627–2634. [CrossRef]
59. Marchetti, F.; Pettinari, R.; Di Nicola, C.; Pettinari, C.; Paul, A.; Crispini, A.; Giorno, E.; Lelj, F.; Stoia, S.; Amati, M. Effect of methyl groups in a pyrimidine-based flexible ligand on the formation of silver(I) coordination networks. *N. J. Chem.* **2018**, *42*, 13998–14008. [CrossRef]
60. Patra, G.K.; Goldberg, I.; De, S.; Datta, D. Effect of the size of discrete anions on the nuclearity of a complex cation. *CrystEngComm* **2007**, *9*, 828–832. [CrossRef]
61. El-Naggar, M.A.; Abu-Youssef, M.A.M.; Soliman, S.M.; Haukka, M.; Al-Majid, A.M.; Barakat, A.; Badr, A.M.A. Synthesis, X-ray structure, Hirshfeld, and antimicrobial studies of new Ag(I) complexes based on pyridine-type ligands. *J. Mol. Struct.* **2022**, *1264*, 133210. [CrossRef]
62. Gotsis, S.; White, A.H. Lewis-Base Adducts of Group-11 Metal(I) Compounds. XXIX. Crystal Structures of Bis(Pyridine-4-carbonitrile)silver(I) Nitrate and Bis(4-benzoylpyridine)Silver(I) Nitrate Monohydrate. *Aust. J. Chem.* **1987**, *40*, 1603–1608. [CrossRef]
63. Song, K.Y.; Zhao, L.M.; Zhang, W.T.; Li, Y.; Li, H.H.; Chen, Z.R. Two-Dimensional Silver-Thiocyanate Layers Directed by Viologens: Structural Transformations upon Low Pressure Stimuli, Piezochromic Luminescence, Photocurrent Responses, and Photocatalytic Properties. *Cryst. Growth Des.* **2018**, *19*, 177–192. [CrossRef]
64. Chakkaradhari, G.; Eskelinen, T.; Degbe, C.; Belyaev, A.; Melnikov, A.S.; Grachova, E.V.; Tunik, S.P.; Hirva, P.; Koshevoy, I.O. Oligophosphine-thiocyanate copper (I) and silver (I) complexes and their borane derivatives showing delayed fluorescence. *Inorg. Chem.* **2019**, *58*, 3646–3660. [CrossRef] [PubMed]
65. Luo, S.Q.; Wang, Q.; Quan, J.; Yang, M.; Wang, Y.; Zhang, X.; Chen, Z.N. A sky-blue luminescent silver (I) complex with a one-dimensional zipper-like structure constructed with 2-diphenylphosphinopyridine and thiocyanate. *Transit. Met. Chem.* **2021**, *46*, 415–421. [CrossRef]
66. Filipović, N.R.; Ristić, P.; Janjić, G.; Klisurić, O.; Puerta, A.; Padron, J.M.; Donnard, M.; Gulea, M.; Todorović, T.R. Silver-based monomer and coordination polymer with organic thiocyanate ligand: Structural, computational and antiproliferative activity study. *Polyhedron* **2019**, *173*, 114132. [CrossRef]
67. Bowmaker, G.A.; Di Nicola, C.; Hanna, J.V.; Healy, P.C.; King, S.P.; Marchetti, F.; Pettinari, C.; Robinson, W.T.; Skelton, B.W.; Sobolev, A.N.; et al. Oligo-nuclear silver thiocyanate complexes with monodentate tertiary phosphine ligands, including novel 'cubane'and 'step'tetramer forms of AgSCN: PR_3 $(1:1)_4$. *Dalton Trans.* **2013**, *42*, 277–291. [CrossRef] [PubMed]
68. Mautner, F.A.; Scherzer, M.; Berger, C.; Fischer, R.C.; Vicente, R.; Massoud, S.S. Synthesis and characterization of five new thiocyanato-and cyanato-metal (II) complexes with 4-azidopyridine as co-ligand. *Polyhedron* **2015**, *85*, 20–26. [CrossRef]
69. Kabesova, M.; Gazo, J. Structure and classification of thiocyanates and the mutual influence of their ligands. *Chem. Zvesti.* **1980**, *34*, 800.
70. Norbury, A.H. Coordination chemistry of the cyanate, thiocyanate, and selenocyanate ions. *Adv. Inorg. Radiochem.* **1975**, *17*, 231–386.
71. Armstrong, D.R.; Khandelwal, A.H.; Raithby, P.R.; Snaith, R.; Stalke, D.; Wright, D.S. Structure of the lithium thiocyanate-tetramethylpropylenediamine complex dimer,$[LiNCS\text{-}Me_2N(CH_2)_3NMe_2]_2$, with asymmetric NCS-bridge bonding: A new bonding mode for the thiocyanate ligand. *Inorg. Chem.* **1993**, *32*, 2132–2136. [CrossRef]
72. Zhu, H.-L.; Liu, G.-F.; Meng, F.-J. Refinement of the crystal structure of silver (I) thiocyanate, AgSCN. *Z. Kristallogr.—N. Cryst. Struct.* **2003**, *218*, 263–264.
73. Luo, G.G.; Sun, D.; Zhang, N.; Huang, R.B.; Zheng, L.S. Two novel silver (I) coordination polymers: Poly [(μ_2-2-aminopyrimidine-κ^2N^1:N^3)bis(μ_3-thiocyanato-κ^3S:S:S)disilver(I)] and poly [(2-amino-4,6-dimethylpyrimidine-κN) (μ_3-thiocyanato-κ^3N:S:S)silver(I)]. *Acta Crystallogr. Sect. C Cryst. Struct. Commun.* **2009**, *65*, m377–m381. [CrossRef] [PubMed]
74. Etaiw, S.E.D.H.; Abd El-Aziz, D.M.; Ibrahim, M.S.; El-din, A.S.B. Synthesis and crystal structures of three novel coordination polymers constructed from Ag (I) thiocyanate and nitrogen donor ligands. *Polyhedron* **2009**, *28*, 1001–1009. [CrossRef]
75. Krautscheid, H.; Emig, N.; Klaassen, N.; Seringer, P. Thiocyanato complexes of the coinage metals: Synthesis and crystal structures of the polymeric pyridine complexes $[Ag_xCu_y(SCN)_{x+y}(py)_z]$. *J. Chem. Soc. Dalton Trans.* **1998**, *18*, 3071–3078. [CrossRef]
76. Sheldrick, G.M. A short history of SHELX. *Acta Cryst. A* **2008**, *64*, 112–122.
77. Turner, M.J.; McKinnon, J.J.; Wolff, S.K.; Grimwood, D.J.; Spackman, P.R.; Jayatilaka, D.; Spackman, M.A. *Crystal Explorer17*; University of Western Australia: Crawley, Australia, 2017.